

Indirect Speed Control Strategy for Maximum Power Point Tracking of the DFIG Wind Turbine System

Estrategia de Control de Velocidad Indirecto para el Seguimiento del Punto Máximo de Potencia de un Sistema Eólico DFIG

E. Ayala¹ S. Simani² N. Pozo³ E. Muñoz⁴

^{1,2,4} Universidad Politécnica Salesiana, Calle Vieja 12-30 and Elia Liut Ave., Cuenca, Ecuador

³ Ferrara University, Via Savonarola, 9, 44121 Ferrara FE, Italy

E-mail: eayala@ups.edu.ec, apozoa@est.ups.edu.ec

silvio.simani@unife.it, emunozp2@est.ups.edu.ec

Abstract

In this article, a control strategy for Maximum Power Point Tracking (MPPT) of a wind turbine system based on a Doubly Fed Induction Generator (DFIG) is presented. The proposed strategy consists of the Indirect Speed Control (ISC) taking the Low Speed Shaft (LSS) as variable input. Even though the pitch control mainly influences the power extraction, this implementation allows the MPPT to optimize the Power Coefficient (C_p) in terms of dynamic response. The controller has been designed in order to allow the wind turbine to reach the MPPT along the partial load operation. For these experiments, a 1.5 MW wind turbine was modeled and simulated by using Matlab and Fatigue, Aerodynamic, Structure and Turbulence (FAST) software. In order to present the achieved results, a comparison between the ISC and a classical PI controller is made. The C_p curves as well as the output power display an important improvement in terms of stability. These results are possible because the appropriate values of optimal Tip Speed Ratio (TSR) and maximum C_p have been properly established.

Resumen

En el siguiente artículo, se propone una estrategia de control para el seguimiento del punto máximo de potencia (MPPT) de un sistema de energía eólica con generador de inducción doblemente alimentado DFIG. La estrategia propuesta está basada en un Control de Velocidad Indirecto (ISC) tomando la velocidad baja del eje como variable de entrada. A pesar que el control de pitch influye principalmente en la extracción de potencia, esta implementación permite realizar un seguimiento del MPPT de modo que el Coeficiente de Potencia (C_p) del sistema se optimice en términos de respuesta dinámica. El controlador ha sido diseñado para permitir que la turbina eólica alcance este punto máximo a lo largo de la zona de operación de carga parcial. Para realizar los experimentos, se seleccionó un aerogenerador de 1,5 MW y el modelo se implementó en una simulación por medio de Matlab y el software de Fatiga, Aerodinámica, Estructuras y Turbulencia (FAST) para el análisis y posterior validación de resultados. La curva de C_p ha sido comparada con un controlador PI mostrando una mejora importante en términos de estabilidad y potencia activa de salida. Estos resultados son posibles debido a que se ha seleccionado apropiadamente los valores de Tip Speed Ratio (TSR) y C_p máximo.

Index terms— Power Coefficient, MPPT, Indirect Speed Control, DFIG, Wind Turbine

Palabras clave— Coeficiente de Potencia, MPPT, Control de Velocidad Indirecto, DFIG, Aerogenerador

Recibido: 29-10-2020, Aprobado tras revisión: 11-01-2021

Forma sugerida de citación: Ayala, E.; Simani, S.; Pozo, A.; Muñoz, E. (2021). "Indirect Speed Control Strategy for Maximum Power Point Tracking of the DFIG Wind Turbine System". Revista Técnica "energía". No. 17, Issue II, Pp. 92-101

ISSN On-line: 2602-8492 - ISSN Impreso: 1390-5074

© 2021 Operador Nacional de Electricidad, CENACE

1. INTRODUCTION

Nowadays, wind energy has grown because of the high demands of renewable energies worldwide. In this context, energy efficiency must be improved in order to obtain as much energy as possible from the source [1], [2], [3]. For wind turbines, the transition from no load to full load operation is crucial for the control of energy production. Particularly, one of the characteristics that allows more energy production is the control strategy during partial load operation also known as MPPT.

The dynamics of the system is one of the most important characteristics because the control strategy is designed by using mechanical and electrical models. The mechanical load must be modeled depending on the number of masses, the gearbox ratio, and the friction losses along the system. With regard to the electric characteristics, the grid connection, the power electronic converter, and the generator losses are included. Although there are different types of electric generators, there are, in the market, there two main popular wind turbines: The Permanent Magnet Synchronous Generator (PMSG) and the Doubly Fed Induction Generator (DFIG). PMSG, which works through a wind turbine, is usually selected for minimizing the cost of maintenance and implementation whereas DFIGs are common for high power applications [4], [5], [6]. The DFIG wind turbine configuration has the advantage of permitting high amounts of power extraction; thus, minimizing the cost of power electronic devices. Further, the control strategy can be widely adjusted since the slip angle is adaptable in a typical range of +/-30% from the operational speed around the synchronous speed [7]. The MPPT control is usually designed by considering the wind speed, rotor speed, output power, and pitch angle. One simple control strategy consists of tracking the electromagnetic torque vs Low Shaft Speed (LSS) curve; thereupon, allowing the system to reach the MPPT using the natural dynamic response. This method is also known as Indirect Speed Control (ISC) [7], [8]. In this article, an ISC strategy for a DFIG wind turbine in order to attain the MPPT is presented. For this simulation, a 1,5MW wind turbine using Matlab and FAST software has been selected [9], [10].

In section two, the analysis and modeling of the subsystems directly involved in the operation of the wind turbine are detailed. Moreover, the parameters of description that have been used for the ISC simulation are explained. In section three, the control strategy and the simulations based on FAST and Simulink are described. Finally, the results are presented in section four.

2. WIND TURBINE MODEL

Basically, the wind turbine transforms the energy of air mass movement into electrical energy. The electromechanical model of the wind turbine depends on the parameters related to the aerodynamics and the size

of the generator. In order to allow the maximum power extraction, it is necessary to obtain the most accurate mathematical model in order to implement an appropriate MPPT control. The most relevant variables involved are the nominal speed of the turbine, the gearbox ratio, the electromagnetic torque of reference, the pitch angle, and the TSR [11], [12], [13]. In Fig. 1, a description of the basic elements of a wind turbine is detailed.

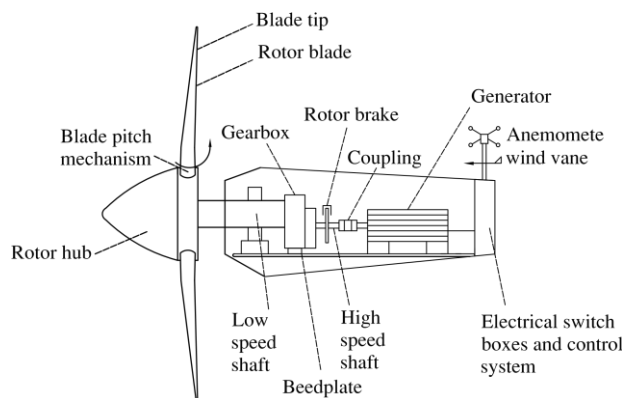


Figure 1: Basic elements of a wind turbine.

2.1 Aerodynamic Model

Aiming to produce the movement of the wind turbine rotor, the air enters the swept rotor area which is a circumference created by the rotation of the blades. The rotor captures the energy of the air, causing a decrease of pressure once the energy is transferred to the mechanism of the wind turbine detailed in Fig. 2 [7].

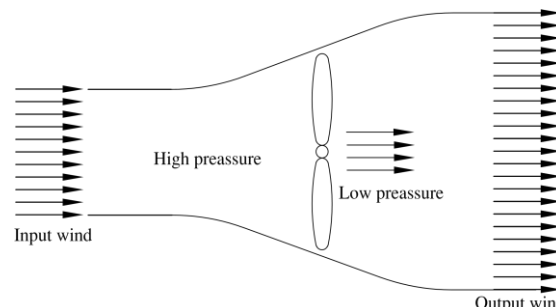


Figure 2: Air flowing through the swept area

The aerodynamic model represents the energy extraction of the rotor, and calculates the mechanical torque as a function of the air flow in each propeller. The wind speed can be considered as the average speed of the incident wind in the area swept by the propellers with the purpose of evaluating the average torque in the low speed axis [5]. The mechanical power can be determined by the expression in equation (1) [1], [3], [14].

$$P_t = \frac{1}{2} \rho A_1 V_v^3 \tag{1}$$

However, the wind turbine can recover only part of available power because of the Betz limit shown in (2). Here is where the term C_p affects the wind turbine performance due to mechanical and electrical losses.



$$P_v = \frac{1}{2} \rho \pi R^2 V_v^3 C_p \quad (2)$$

Where, R is the wind turbine blade radius, ρ is the air density, V_v is the wind speed, and C_p is the power coefficient.

For a wind turbine, Betz's law establishes that 59.26% of the kinetic energy of the wind can be converted into useful mechanical energy [7]. The other losses of the system described by the parameter C_p are defined by the relationship in (3).

$$C_p = \frac{P_t}{P_v} < 59.26\% \quad (3)$$

For a wind turbine, C_p is, on a regular basis, experimentally by the manufacturers. The C_p depends on TSR and pitch angle β described in equation (4). The general equation (5) makes reference to the family of curves that relates TSR to C_p of a wind turbine [7], [13].

$$\lambda = \frac{R \cdot \Omega_t}{V_v} \quad (4)$$

$$C_p = c_1 \cdot \left[\frac{c_2}{\lambda_i} - c_3 \beta - c_4 \right] e^{-\frac{c_5}{\lambda_i}} + c_6 \lambda \quad (5)$$

Where

$$\lambda_i = \left[\frac{1}{\lambda + c_7 \beta} - \frac{c_8}{(\beta^3 + 1)} \right]^{-1} \quad (6)$$

2.2 Mechanical Model

For the mechanical model, the two-mass representation of the speed joint in the power transmission and linked to the gearbox which transmits the torque caused by the impact of the wind has been modeled in this work. The mechanical model is displayed in Fig. 3.

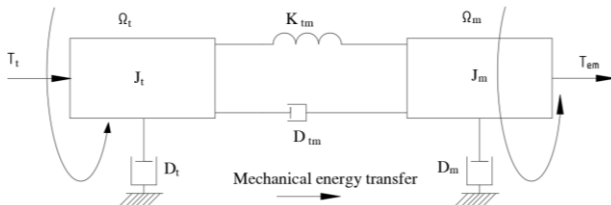


Figure 3: Two-mass mechanical model

The left side of Fig. 3 represents the low-speed part, where the propellers are generating the low-speed rotational movement. On the right, the high-speed side which is attached to the generator rotor is located. The moment of inertia and torque are detailed in equations (7) [5], [7].

$$\begin{aligned} J_t \frac{d\Omega_t}{dt} &= T_t - D_t \Omega_t - T_{em} \\ J_m \frac{d\Omega_m}{dt} &= T_{em} - D_m \Omega_m + T_{em} \\ \frac{dT_{em}}{dt} &= K_{tm} (\Omega_t - \Omega_m) + D_{tm} \left(\frac{d\Omega_t}{dt} - \frac{d\Omega_m}{dt} \right) \end{aligned} \quad (7)$$

Where:

Ω_t = Low Shaft Speed LSS

Ω_m = High Shaft Speed HSS

The model can be simplified by discarding the damping coefficients (D_t , D_m , and D_{tm}); hence, resulting in a two-inertia model (J_t and J_m) and the stiffness constant (K_{tm}).

2.3 Pitch Control Model

The objective of the controller is to manipulate the pitch of the propellers at different angles to increase or decrease the wind turbine speed. The β -pitch controllers allow independent control of each propeller usually through hydraulic actuators. This permits the reduction of the tension generated in the entire system. Pitch angle regulation is modeled, as shown in Fig. 4, by a PI controller which generates a reference rate. This reference is limited, and a first order system provides the dynamic behavior of the speed control of the wind variation. The angle of inclination itself is then obtained by integrating the variation of the angle. The control of a variable-speed wind turbine is needed to calculate both the generator torque and the pitch angle references in order to comply with the generator speed regulation [7].

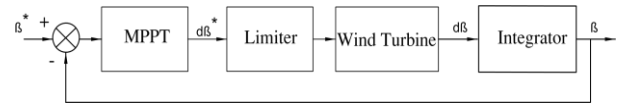


Figure 4: Pitch angle control system

2.4 Wind Turbine Speed Control

The wind turbine benchmark is oriented to design high power systems (1 MW onwards). For such applications, DFIGs are popular as they can generate high controllable power thanks to the size of the power electronics converters compared to other wind turbine technologies [7], [15]. For instance, it can be seen, in Fig. 5, a general control scheme for the operation of the Wind Turbine at variable speed, where there are two important input signals for the controllers: the generator electromagnetic reference torque and the pitch angle command.

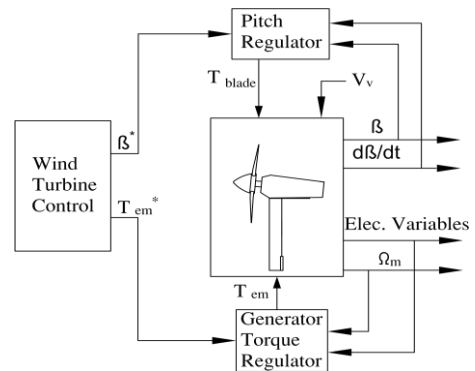


Figure 5: Wind turbine

The main goal is to extract the maximum energy from the wind, keep the wind turbine in a safe operating mode (power, speed and torque below limits), and mechanical stress reduction on the drivetrain. The turbine control operation zones used in the development of this work is illustrated in Fig. 6 and consists of four areas of operation [7] where four zones are displayed: 1) Minimum operating speed zone restriction, 2) MPPT zone into partial load operation for variable speed operation until nominal speed is achieved, 3) the maximum speed in partial load operation and 4) full load operation before the brake is applied. The objective of the proposed controllers is to regulate the operation of the wind turbine so that it works in its second operating zone, this will allow obtaining the maximum power monitoring.

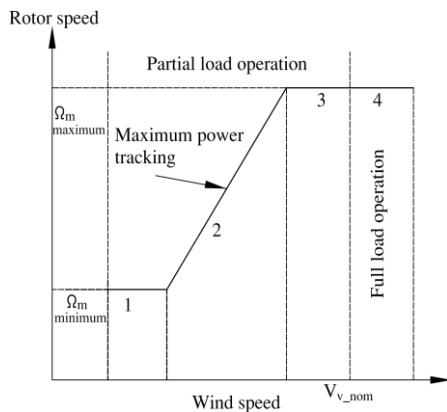


Figure 6: Operation zones of the wind turbine description

3. INDIRECT SPEED CONTROL STRATEGY

The indirect speed control strategy is based on the relationship between the electromagnetic torque T_{em} and the angular velocity Ω_t . Nonetheless, the relation between the electromagnetic torque and the angular velocity does not have a direct dynamic relationship due to the inertia involved. This leads to a much slower response of the system as the mechanical coupling is not canceled [7]. The ISC modifies the dq frame currents in order to command the back to back converter allowing the controllability of the slip angle which also affects the speed and torque of the generator. The scheme to be implemented is shown in Fig. 7.

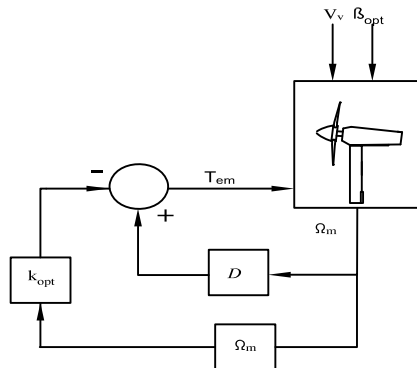


Figure 7: Indirect Speed Control strategy general block diagram

When the wind turbine operates at optimal conditions, the parameters allow finding a constant value called k_{opt} which is used for the optimal electromagnetic torque reference calculation. The general description can be found in equations (8). According to [7], the ISC can be achieved by measuring the LSS and subtracting the mechanical losses as shown in Figure. 7. The Electromagnetic torque of reference T_{em} is calculated in terms of k_{opt} and the LSS Ω_m . In equation (9) and (10), it is shown how the k_{opt} is determined. The ISC strategy also considers the mechanical losses at the gearbox established at block D including friction and damping factors [13], [16].

$$\lambda_{opt} = \frac{R\Omega_m}{V_v}; C_p = C_{p_max}; \text{ y } C_t = C_{t_max} \quad (8)$$

$$T_{em} = \frac{1}{2} \rho \pi \frac{R^5}{\lambda_{opt}^3} C_{p_max} \Omega_m^2 = k_{opt} \Omega_m^2 \quad (9)$$

$$k_{opt} = \frac{1}{2} \rho \pi \frac{R^5}{\lambda_{opt}^3} C_{p_max} \quad (10)$$

For k_{opt} calculation it is necessary to establish the optimal TSR λ_{opt} and the corresponding C_{p_max} . These parameters can be either calculated experimentally or provided by the manufacturer. In this work, multiple simulations using Matlab and FAST were used to estimate λ_{opt} , C_{p_max} and compared to manufacturers specifications found in [17] (see Table 1).

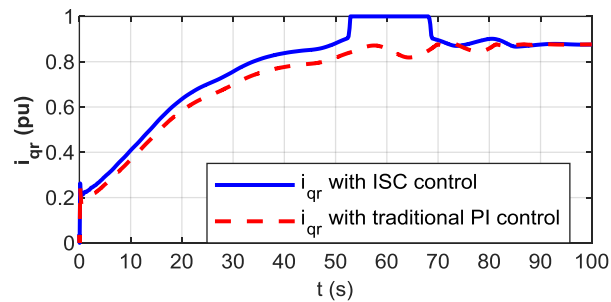
Table 1: Parameters for Iqr calculation

| Parameter | Value | Description |
|-----------------|-----------------|--------------------------------|
| C_{p_max} | 0,5 | Maximum Power Coefficient |
| Air density | 1,225 | Air density configured to FAST |
| R | 41,25 | Blade lenght |
| λ_{opt} | 7,4 | Optimal Tip Speed Ratio |
| N | 72 | Gearbox ratio |
| LSS | Input variable | Low Shaft Speed |
| wr | Input variable | Angular rotor speed |
| Power | Input variable | Output power |
| iqr* | Output variable | Reference current iq |

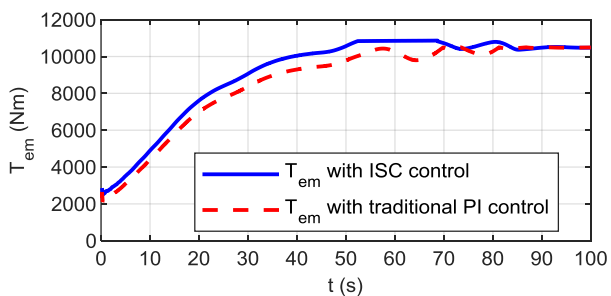
3.1 Indirect Speed Control Implementation

FAST models a wind turbine as a composition of rigid and flexible elements. For example, two-blade turbines are modeled as four rigid and four flexible bodies. The rigid bodies are the ground, the nacelle, the hub, and the tip brakes (point masses) whereas flexible bodies comprise blades, tower, and transmission system. The components of both flexible and rigid bodies include the following variables: tower bending, blade bending, nacelle yaw, rotor position, rotor speed, and driveshaft torsional flexibility. The tower bending has two modes, each in the front-to-back and side-to-side directions, and flexible blades have two modes of rotation and one edge per blade mode. In Fig. 8, the FAST model [18] implemented in Simulink [10] can be observed to obtain a matrix of output variables which directly interact in the proposed controller model.

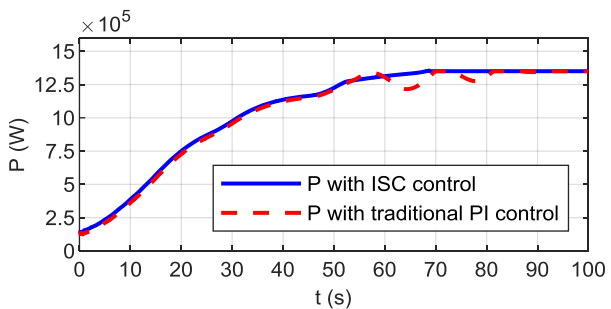
attained, the output power reaches near 1,5MW, and these wind speed profiles generate a stable C_p near 0,5. In terms of the pitch controller, it also operates, but the simulations are intended to reduce its direct influence over the MPPT controller. In this test, the main achievement is the stability of the C_p signal in Fig. 10 (g), the ISC MPPT can be observed even though the C_p average value has short increase. However, the output power shown in Fig. 10 (c) also describes a small increment in level an also stability. Fig 10 (a) shows the i_{qr} reference current in per units which is similar for both controllers, however, for the ISC the current is saturated between 50 and 70 seconds because the wind speed is over the partial load limit. For this experiment, pitch angle controller is activated when the magnitude of the wind is above 9,5 m/s which corresponds to the manufacturer specifications. The pitch angle can be observed in Fig. 10 (f) where the pitch angle executes three corrections before the steady state for traditional PI control and two corrections for the case of the ISC. This leads to a less pitch dependent approach reducing the stress of the components of the overall system.



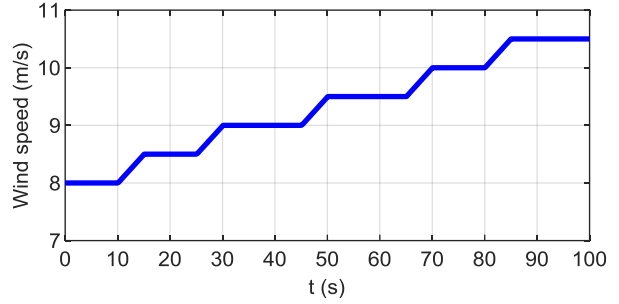
(a)



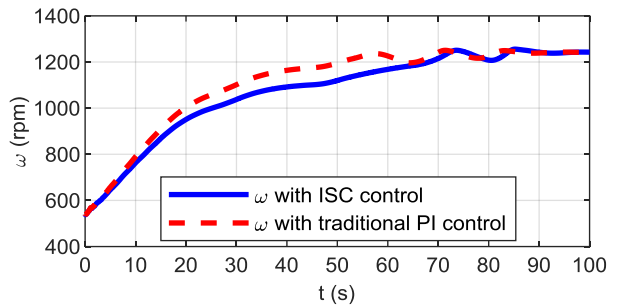
(b)



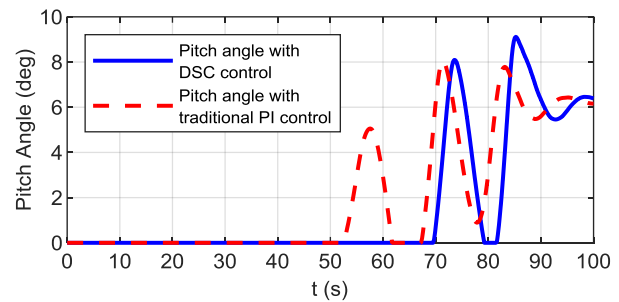
(c)



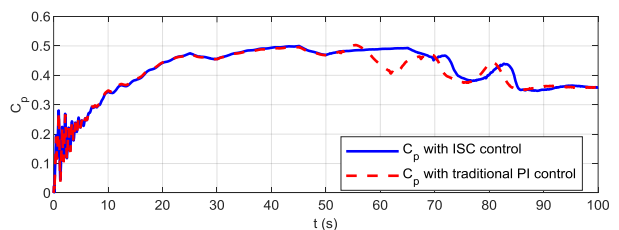
(d)



(e)



(f)



(g)

Figure 10: Steady wind speed with ramp type transitions: Reference signal i_{qr} in p.u. (a), electromagnetic torque in Nm (b), active output power in W (c), wind input in m/s (d), generator speed in rpm (e), pitch angle in degrees (f) and C_p (g)

4.2 Variable wind speed with positive and negative ramps

The second wind speed signal used for simulations consists of a variable wind speed with triangular type signal. The idea, here, is to test the system with a more realistic oscillatory signal in order to evaluate the dynamic response using triangular input winds. This signal simulates an increasing wind speed profile which



varies between 6,5 and 8,5 m/s. To comply with the study's guidelines, 100 seconds of simulation have been tested. The power remains about 0,9 MW in average during MPPT zone. It is fundamental to emphasize that even though the wind turbine has been configured at the rated speed of 11 m/s, the simulation is intended to evaluate the dynamic response during the variations of wind. Moreover, although the initial inertia and torque are low for testing the dynamics during partial load, a very strong oscillation at the beginning of the simulation which corresponds to the initial inertia configuration in FAST can be observed. When the rated speed is attained, the output power reaches near 0,75 MW, and the wind speed profiles generate a stable C_p near 0,5. With respect to the pitch controller, it also acts when the wind speed increases, and because of this, the system is tested mainly during partial load without a straight impact of pitch control. In Fig. 11 (a) it is shown the triangular input signal with small slopes starting with 7 m/s speed. For this experiments the pitch angle does not actually work because the wind speed is low as shown in Fig. 11 (f). The output power clearly increases after 80 seconds and remains higher for a steady state condition after 90 seconds as shown in Fig. 11 (c). Iqr displays smooth variations following the response of the wind in the triangular shape function.

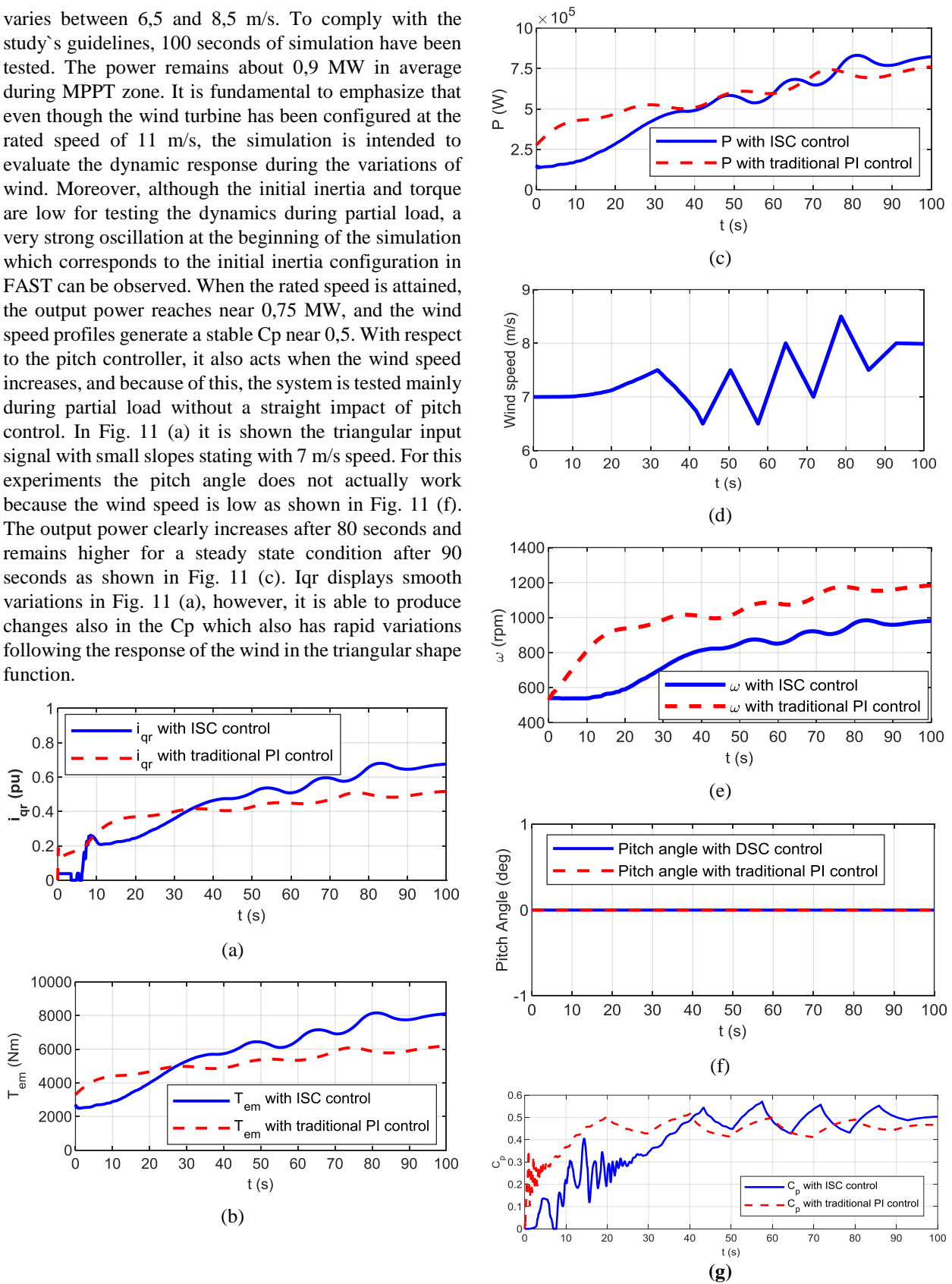
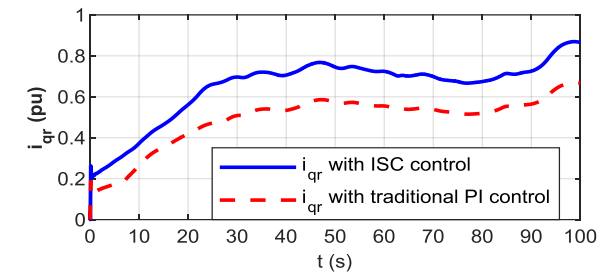


Figure 11: Steady wind speed with positive and negative ramp: Reference signal i_{qr} in p.u. (a), electromagnetic torque in Nm (b), active output power in W (c), wind input in m/s (d), generator speed in rpm (e), pitch angle in degrees (f) and C_p (g)

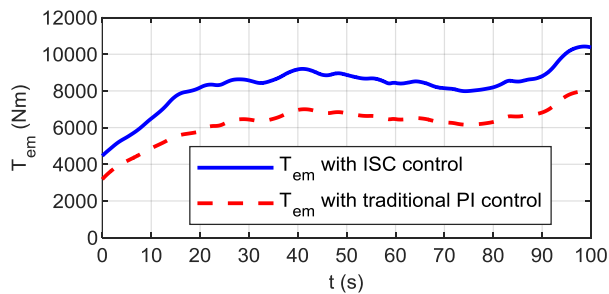


4.3 Variable Wind Speed with realistic input

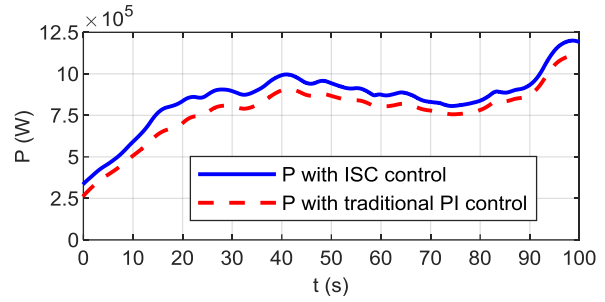
The third wind speed signal used for simulations consists of a variable wind speed with transitions. The idea, here, is to test the system with a more realistic oscillatory signal in order to evaluate the dynamic response. The oscillatory signal simulates an increasing wind speed profile which varies from 7 to 10 m/s. Thereupon, 100 seconds of simulation have been tested. Under those circumstances, the following results were obtained. First, the output power remains about 0,9MW in average during MPPT zone. At this instant, it is important to highlight that even though the wind turbine is at rated speed of 11 m/s, the simulation only considers the partial load and the initial conditions. Moreover, the initial inertia and torque are low for testing the dynamics during partial load. When the rated speed is attained, the output power reaches near 1,25MW due to the slip, and these wind speed profiles generate a stable C_p near 0,5. Regarding the pitch controller, it also acts when the wind speed increases, and because of this, the system is tested mainly during partial load without a straight impact of pitch control. The generated realistic input wind speed can be observed in Fig. 12 (d). The improvements of the C_p are observed in Fig. 12 (g) along basically all the curve. The pitch angle also remains zero because of the range of the wind speed as shown in Fig. 12 (f). Probably the best outcome during this experiment is the improvement of the output power along the curve following the variations of the inputted wind.



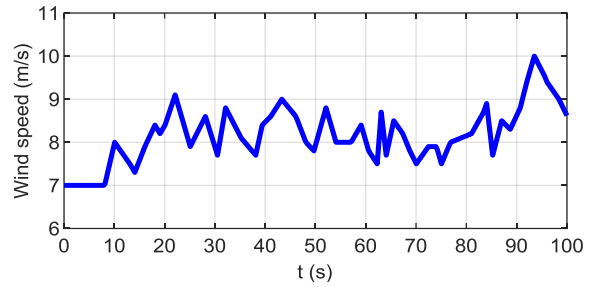
(a)



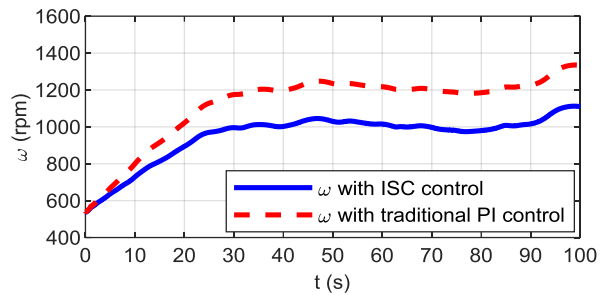
(b)



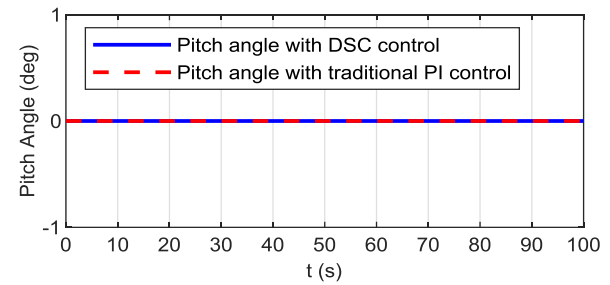
(c)



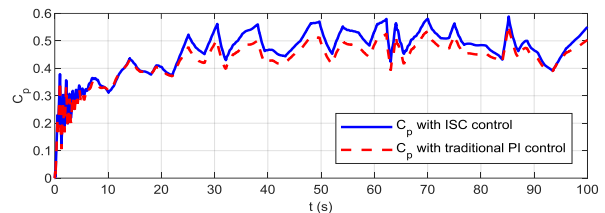
(d)



(e)



(f)



(g)

Figure 12: Steady wind speed with realistic inputs: Reference signal i_{qr} in p.u. (a), electromagnetic torque in Nm (b), active output power in W (c), wind input in m/s (d), generator speed in rpm (e), pitch angle in degrees (f) and C_p (g)

5. CONCLUSIONS

In this work, the ISC has been implemented by using FAST and Matlab for a DFIG 1,5MW wind turbine. Compared to the classical PI control, the results display an important improvement because of the correct selection of optimal TSR and maximum C_p when calculating the optimal constant at the controller stage. This implementation also considers the initial LSS speed and inertia which produce an oscillation during the first 20 seconds of simulation. Nevertheless, after that period of time, the rotor speed becomes steady and close to the nominal value. The aforementioned tests have the intention of demonstrating the capability of this technique for responding fast, even for disturbed wind input. Furthermore, the pitch control is able to perform a correct control for limiting the speed of the shaft. This is important since the C_p performance is also affected by the pitch angle. After the simulation enters a full load operation, the power and speed become nominal values, but in these experiments, the idea is to demonstrate the correct operation of the wind turbine along the partial load operation.

The DFIG electric machine could also have a different configuration for the connection to the grid; thus, allowing the system to provide more power depending on the active and reactive power. The ISC improvements compared with traditional PID controllers can be quantified in terms of stability but mainly of C_p maximization. This can be observed in the results when the average output active power is measured where the ISC allows more power extraction. Because of the nature of the wind turbine components, the dynamic error represents all possible stages of the wind turbine where the energy is transformed. The variations in the wind speed input produces many transients over the output power and power coefficient consequently. The wind speed is not usually constant for real scenarios and it is mostly considered as an oscillatory signal which produces a complex dynamic. The ISC could be improved when the knowledge of all possible variables is available since it is very sensitive to disturbances and implementation of DSC methods are recommended for better dynamic performance.

REFERENCES

- [1] E. Rahmanian, H. Akbari y H. Sheisi, «Maximum Power Point Tracking in Grid Connected Wind Plant by Using Intelligent Controller and Switched Reluctance Generator,» *IEEE Transactions on Sustainable Energy*, vol. 8, n° 3, pp. 1313-1320, 2017.
- [2] J. Singh Thongam y . M. Ouhrouche, «MPPT Control Methods in Wind Energy Conversion Systems,» *Fundamental and Advanced Topics in Wind Power*, pp. 339-360, 2011.
- [3] J. Mohammadi, S. Vaez-Zadeh, . S. Afsharnia y E. Daryabeigi, «A Combined Vector and Direct Power Control for DFIG-Based Wind Turbines,» *IEEE Transactions on Sustainable Energy*, vol. 5, n° 3, 2014.
- [4] W. Hofmann y F. Okafor, «Doubly-fed full-controlled induction wind generator for optimal power utilisation,» *4th IEEE International Conference on Power Electronics and Drive Systems*, vol. 1, pp. 355-361, 2001.
- [5] M. Hallak, M. Hasni y M. Mena, «Modeling and Control of a Doubly Fed Induction Generator Base Wind Turbine System,» *3rd CISTEM'18*, 2018.
- [6] E. Ayala y S. Simani, «Perturb and observe maximum power point tracking algorithm for permanent magnet synchronous generator wind turbine systems.,» *Proceedings of the 15th European Workshop on Advanced Control and Diagnostics.*, pp. 1-11, 2019.
- [7] G. Abad, J. Lopez, R. A. Miguel, L. Marroyo y G. Iwanski, *Doubly Fed Induction Machine*, WILEY, 2011.
- [8] K. Bedoud, M. Ali-rachedi, T. Bahi, R. Lakel y A. Grid, «Robust Control of Doubly Fed Induction Generator for Wind Turbine Under Sub-synchronous Operation Mode,» *Energy Procedia*, vol. 74, pp. 886-899, 2015.
- [9] National Renewable Energy Laboratory (NREL), *Fatigue Aerodynamics Structures and Turbulence*, 2020.
- [10] The MathWorks Inc., *Matlab*, Massachusetts.
- [11] E. Tremblay, S. Atayde y A. Chandra, «Direct Power Control of a DFIG-based WECS with Active Filter Capabilities,» *IEEE Electrical Power and Energy*, 2009.
- [12] D. Petković, Ž. Čojbašić, V. Nikolić, S. Shamshirband, M. L. M. Kia, N. B. Anuar y A. W. A. Wahab, «Adaptive neuro-fuzzy maximal power extraction of wind turbine with continuously variable transmission,» *Energy*, vol. 64, pp. 868-874, 2014.
- [13] Q. Wang y L. Chang, «An Intelligent Maximum Power Extraction Algorithm for Inverter-Based Variable Speed Wind Turbine Systems,» *IEEE Transactions on Power Electronics*, vol. 19, n° 5, p. 1242:1249, 2004.
- [14] N. Mendis, K. Muttaqi, S. Sayeef y S. Perera, «Standalone Operation of Wind Turbine-Based Variable Speed Generators With Maximum Power

Extraction Capability,» IEEE Transactions on Energy Conversion, vol. 27, n° 4, pp. 822-834, 2012.

- [15] S. Muller, M. Deicke y D. R. W., «Doubly Fed Induction Generators Systems for Wind Turbines,» IEEE Industry Applications, vol. 8, n° 3, pp. 26-33, 2000.
- [16] G. Abad, «Properties and Control of a Doubly Fed Induction Machine,» de Power Electronics for Renewable Energy Systems, Transportation and Industrial Applications, IEEE, 2014, pp. 270-318.
- [17] C. Carrillo, A. F. Obando Montaña, J. Cidrás y E. Diaz, «Review of power curve modelling for wind turbines,» Renewable and Sustainable Energy Reviews, vol. 21, pp. 572-581, 2013.
- [18] NREL, Simulation for Wind Turbine Generators—With FAST and MATLAB-Simulink Modules, United States: NREL, 2014.
- [19] M. Singh, E. Muljadi, J. Jonkman, I. Girsang y J. Dhupia, Simulation for Wind Turbine Generators—With FAST and MATLAB-Simulink Modules, NREL, 2014.



Nicolás Pozo Ayala.- Nació en Cuenca, Ecuador en 1998. Es estudiante de Mecatrónica con mención en Automatización Industrial desde el año 2016 en la Universidad Politécnica Salesiana. Sus áreas de estudios se focalizan en la automatización de procesos alimenticios y desarrollo de dispositivos para personas con discapacidad.



Eduardo Muñoz Palomeque.- Nació en Cuenca, Ecuador en 1997. Actualmente, se encuentra culminando sus estudios de grado en la carrera de Ingeniería Mecatrónica en la Universidad Politécnica Salesiana Sede Cuenca del Ecuador. Sus intereses en áreas de investigación incluyen técnicas de procesamiento de señales, sistemas autónomos y electrónica de potencia.



Edy Ayala Cruz.- Nació en Cuenca en 1987. Recibió su título de Tecnólogo Electrónico en 2009 y de Ingeniera Electrónico en 2011, ambos de la Universidad Politécnica Salesiana del Ecuador; y su título de Máster of Engineering Science (Electrical and Electronic)

de Swinburne University of Technology en Australia, 2015. Actualmente, se encuentra cursando sus estudios de Doctorado en Ingeniería en la Universidad de Ferrara. Su campo de investigación se encuentra relacionado con sistemas de control en ingeniería y energías renovables.



Silvio Simani.- Nació en Ferrara, Italia en 1971. Obtuvo su título en Ingeniería Eléctrica por la Università Degli Studi Di Ferrara (Italia) en 1996; y su Ph.D. en Ciencias de la Información: Control Automático de la Universidad de Ferrara y Modena

(Italia). Sus intereses de investigación incluyen el diagnóstico de fallas de procesos dinámicos, el modelado e identificación de sistemas y los problemas de interacción entre la identificación y el diagnóstico de fallas.